Inclusion of Structural Flexibility in Design Load Analysis for Wave Energy Converters

Yi Guo
National Renewable Energy Laboratory
15013 Denver W Pkwy, Golden, CO, 80401, United States
E-mail: yi.guo@nrel.gov

Yi-Hsiang Yu
National Renewable Energy Laboratory
15013 Denver W Pkwy, Golden, CO, 80401, United States
E-mail: Yi-Hsiang.Yu@nrel.gov

Jennifer van Rij
National Renewable Energy Laboratory
15013 Denver W Pkwy, Golden, CO, 80401, United States
E-mail: jennifer.vanrij@nrel.gov

Nathan Tom
National Renewable Energy Laboratory
15013 Denver W Pkwy, Golden, CO, 80401, United States
E-mail: Nathan Tom@nrel.gov

***Abstract*—Hydroelastic interactions, due to ocean wave loading on wave energy devices with deformable structures, are studied in the time domain. A mid-fidelity, hybrid modeling approach of rigid-body and flexible-body dynamics is developed and implemented in an open-source simulation tool for wave energy converters (WEC), WEC-Sim, to simulate the dynamic responses of WEC component structural deformations under wave loading. A generalized coordinate system, including degrees of freedom associated with rigid bodies, structural modes, and constraints connecting multiple bodies, is utilized. A simplified method of calculating stress loads and sectional bending moments is implemented, with the purpose of sizing and designing WECs. Results calculated using the method presented are verified with those of high-fidelity fluid-structure interaction simulations, as well as low-fidelity, frequency-domain, boundary element method analysis.**

***Index Terms*—Wave energy converter, structural flexibility, design, dynamics, and modal analysis**

I. Introduction

Harvesting energy from the ocean has attracted increased research attention in the recent decades [1], [2]. Numerous forms of WECs have been designed to capture the energy of the ocean surface waves and convert it to electricity [3]. Compared to other renewable energy sources, such as wind and solar, the wave energy resource is less seasonal and offers the highest energy density [4]. However, wave energy technologies are still in the early stages of research and a physical understanding for optimizing WEC reliability and lowering the cost of energy is still evolving.

Structural costs have been identified as one of the primary cost drivers for WECs. Indicating that, accurate load predictions during the design process are essential to further reduce the cost of WECs. Furthermore, several new concepts incorporating composite materials and flexible WEC components, rather than the traditional steel/rigid-body designs, have recently been proposed as a potential cost reduction pathway. Consequently, WEC structural flexibility, as well as the resulting fluid structure interactions (FSI) of the WEC system, have become increasingly important aspects to WEC design. Therefore, in considering the interaction between wave loading and WEC structural dynamics, an accurate and computationally efficient coupled approach for structural and hydrodynamic analyses is highly desired for WEC design.

The most widely used approach for FSI modeling is to couple computational fluid dynamics with finite element analysis. Another direct method to modeling the structural-hydrodynamic behavior of flexible WEC components is to simultaneously model the frequency-domain hydrodynamic boundary value problem with the elastic finite element response [5]. However, both approaches are computationally expensive and generally unsuitable in the initial phases of WEC design. Alternatively, a reduced-order, generalized modes method may be adopted, in which additional degrees of freedom (DOF) associated with a preselected set of generalized body modes, are included in the frequency-domain hydrodynamic boundary value problem [6]. These generalized modes are typically the natural mode shapes of the deformable structures, however, approximate mode shapes, such as Legendre polynomials may also be used [6]. Hydrodynamic loads corresponding to radiation (i.e. added mass and damping coefficients) and wave excitation are then evaluated based on a unit modal response. Newman used the generalized modes method to analyze the deformation of barges and a vertical cylinder using WAMIT, a frequency-domain, boundary-element-based potential flow solver [6], [7]. A similar study was conducted to analyze a very flexible barge in the time-domain utilizing hydrodynamic coefficients from a frequency domain potential flow solution and a state-space model to approximate the radiation and excitation impulse response functions [8]–[10].

The objective of this research is to use and verify the generalized modes method to calculate wave induced structure loads and flexible body dynamics for WEC applications. In this study, the generalized modes method is adopted in WEC-Sim, a radiation-diffraction-based time-domain numerical model that calculates the dynamics of WEC devices comprised of rigid bodies, power-take-off systems, and mooring systems [11]. The generalized modes method is also used to recover

ISSN 2309-1983

body component stress and bending moments, using an approach based on the linear superposition of stresses/bending moments in modal coordinates [12]. The modal stresses/ bending moments corresponding to the component modes can be calculated either analytically or by finite element analyses (FEA). After describing the process of implementing modes derived from FEA, and the dynamics model used to combine rigid and flexible body simulations, the resulting numerical method is applied to simulate a barge and a vertical cylinder, the results of which are compared to high-fidelity coupled hydro-elastic simulations. Finally, future research applications for the generalized body modes methods, including mooring and PTO, are discussed.

II. Component Specifications

Two flexible structures are considered in this study, a barge and a column, each of which are based on Newman's original examples in [6] and further considered in [1]. Both structures may be considered as simplified representations of WEC components - a "Wave-Carpet"-type device, and a monopile for a single-body-point-absorber. Parameters for these structures are listed in Table I.

TABLE I
PARAMETERS FOR THE BARGE AND COLUMN

Property	Units	Barge	Column
Mass	kg	4.000×10^6	3.142×10^7
Density	kg/m^2	500.000	500.000
Cross Sectional Area	m^2	100.000	341.159
Young's Modulus	MPa	30.720	4800.000
Area moment of inertia	m^2	833.333	7853.982
Length	m	80.0	200.0
Poisson's ratio	–	0.3	0.3

III. Flexible Multibody Dynamic Modeling

This section describes the formulation used to model flexible multibody dynamics for WEC devices. The system considers both the rigid-body motions and the structural deformations of WEC components. The dynamic, structural deformations of WEC bodies are evaluated in modal coordinates while rigid body dynamics is calculated in physical coordinates. Assuming the rigid-body motions may be decoupled from the structural deformation significantly reduces computation time and modeling complexity. With the assumption of linear structure with small deformation, the modal properties of flexible bodies may be simply obtained with closed-form analytic expressions or finite element analysis; and the rigid body system is discretized using a classical rigid body dynamics approach. The resulting dynamic response of the WEC device then combines the rigid body motions with the flexible deformations.

The equation of motion of the hydro-elastic-multibody dynamics of WEC is formulated as

$$(\mathbf{M}+\mathbf{A}_\infty)\ddot{\mathbf{x}}+\int_0^t \mathbf{D}(t-\tau)\dot{\mathbf{x}}(\tau)d\tau \quad +\mathbf{C}\dot{\mathbf{x}}-\tfrac{1}{2}\rho A C_D\dot{\mathbf{x}}|\dot{\mathbf{x}}|+ \mathbf{K}\mathbf{x}=\mathbf{F} \tag{1}$$

where $\mathbf{C}=\mathbf{C}_M+\mathbf{C}_{PTO}+\mathbf{C}_{ld}+\mathbf{C}_s$, $\mathbf{K}=\mathbf{K}_M+\mathbf{K}_{PTO}+\mathbf{K}_B+\mathbf{K}_s$, and $\mathbf{F}=\mathbf{F}_{ext}+\mathbf{F}_{ME}$. Throughout the paper, $\mathbf{M}$, $\mathbf{C}$, $\mathbf{K}$ denotes mass, damping, and stiffness matrices. $\mathbf{F}$ is the excitation force vector. The subscripts f, r, and s stand for rigid body, flexible body, and their hybrid system respectively. Subscripts M, PTO, ME, ext, B denote mooring, power take off, Morison, excitation, and Buoyancy. $\mathbf{A}_\infty$ is the added mass terms for the structure.

$$\mathbf{M}=diag\left[\mathbf{M}_{r,1},\overline{\mathbf{M}}_{f,1},\mathbf{M}_{r,2},\overline{\mathbf{M}}_{f,2},\ldots,\overline{\mathbf{M}}_{f,N}\right] \tag{2}$$

$$\mathbf{K}_s=diag\left[\mathbf{K}_{r,1},\overline{\mathbf{K}}_{f,1},\mathbf{K}_{r,2},\overline{\mathbf{K}}_{f,2},\ldots,\overline{\mathbf{k}}_{f,N}\right] \tag{3}$$

$$\mathbf{C}_s=diag\left[\mathbf{C}_{r,1},\mathbf{0},\mathbf{C}_{r,2},\mathbf{0},\ldots,\mathbf{C}_{r,N},\mathbf{0}\right] \tag{4}$$

$$\mathbf{F}=\left[\mathbf{F}_{r,1},\overline{\mathbf{F}}_{f,1},\mathbf{F}_{r,2},\overline{\mathbf{F}}_{f,2},\ldots,\mathbf{F}_{r,N},\overline{\mathbf{F}}_{f,N}\right] \tag{5}$$

where $\overline{\mathbf{M}}_f=\mathbf{\Phi}^T\mathbf{M}_f\mathbf{\Phi}$ and $\overline{\mathbf{K}}_f=\mathbf{\Phi}^T\mathbf{K}_f\mathbf{\Phi}$ are diagonal matrices. Excitation force in the modal coordinates is $\overline{\mathbf{F}}_f=\mathbf{\Phi}^T\mathbf{F}_f$.

Here, $\mathbf{x}=\{\mathbf{z}_1,\mathbf{z}_2,...,\mathbf{z}_N\}^T$ Where N is the total number of bodies in the system. Each displacement vector consists of rigid and flexible DOFs as

$$\mathbf{z}=\{\mathbf{p},\mathbf{q}\}=\{\underbrace{x,y,z,\theta_x,\theta_y,\theta_z}_{\text{Rigid}},\underbrace{q_1,q_2,\ldots,q_m}_{\text{Flexible}}\} \tag{6}$$

In the system environment m is user-defined variable depending on the body selection. In other words, the number of flexible modes for each body can be different. The total DOFs for the system, therefore, equals $6N+\sum_{j=1}^{N}m(j)$ including $6N$ rigid body DOFs and $\sum_{j=1}^{N}m(j)$ flexible body DOFs .

Assuming the dynamic response $\mathbf{u}$ is the linear superposition of system's eigenvectors, such as

$$\mathbf{u}=\mathbf{\Phi}\mathbf{q} \tag{7}$$

where $\mathbf{q}=\{q_1,q_2,\ldots,q_m\}^T$, $\mathbf{\Phi}=[\Phi_1,\Phi_2,\ldots,\Phi_m]$ and m is the total number of eigenvectors.

Similar to Eq. 7, the dynamic stress response of any flexible WEC body, $\mathbf{\Xi}$, is the linear superposition of system's stress distribution in the modal coordinate, such as

$$\mathbf{\Xi}=\mathbf{\Upsilon}\mathbf{q} \tag{8}$$

where $\mathbf{\Upsilon}$ is the stress vector of the flexible body in the modal coordinates.

The bending moment of the same flexible body, $\mathbf{T}$, is

$$\mathbf{T}=\mathbf{\Lambda}\mathbf{q} \tag{9}$$

where $\mathbf{\Lambda}$ is the bending moment vector of the flexible body in the modal coordinate.

In WEC-Sim, the Eq. 1 has been formulated in a state-space form as follows

$$\dot{\mathbf{y}} = \underbrace{\begin{bmatrix} \mathbf{0}, & \mathbf{I} \\ -\mathbf{M}^{-1}\mathbf{K}, & -\mathbf{M}^{-1}\mathbf{C} \end{bmatrix}}_{\mathbf{AA}} \mathbf{y} + \underbrace{\begin{bmatrix} \mathbf{0} \\ \mathbf{M}^{-1}[\mathbf{A}_\infty \ddot{\mathbf{x}} - \int_0^t \mathbf{D}(t-\tau)\dot{\mathbf{x}}(\tau)d\tau + \\ \frac{1}{2}\rho A C_D \dot{\mathbf{x}}|\dot{\mathbf{x}}| + \mathbf{F}_{ext} + \mathbf{F}_{ME}] \end{bmatrix}}_{\mathbf{BB}(t)} \quad (10)$$

where $\mathbf{y} = [\mathbf{x}; \dot{\mathbf{x}}]^T$. $\mathbf{AA}$ is time-invariant coefficient matrix. $\mathbf{BB}$ is time-varying excitation vector. Terms $\mathbf{A}_\infty \ddot{\mathbf{x}}$, $\int_0^t \mathbf{D}(t-\tau)\dot{\mathbf{x}}(\tau)d\tau$, and $\frac{1}{2}\rho \mathbf{A}_D \dot{\mathbf{x}}|\dot{\mathbf{x}}|$ are approximated using solutions at previous time steps. Eq. 10 is solved using ODE4 in Matlab.

The proposed modeling approach has been implemented in WEC-Sim. Solving WEC dynamic response consists of multiple major steps including 1), modal analysis of the studied WEC to identify a set of system natural frequencies and corresponding mode shapes; 2) construct discretized mass and impedance matrices using these structural modes; 3) include these additional degrees of freedom in WAMIT as generalized modes to calculate the additional hydrodynamic coefficients to capture the structural-fluid interaction; and 4) import the hydrodynamic coefficients to WEC-Sim and conduct dynamic analysis of the hybrid rigid and flexible body system. These key steps are also illustrated in Fig. 4.

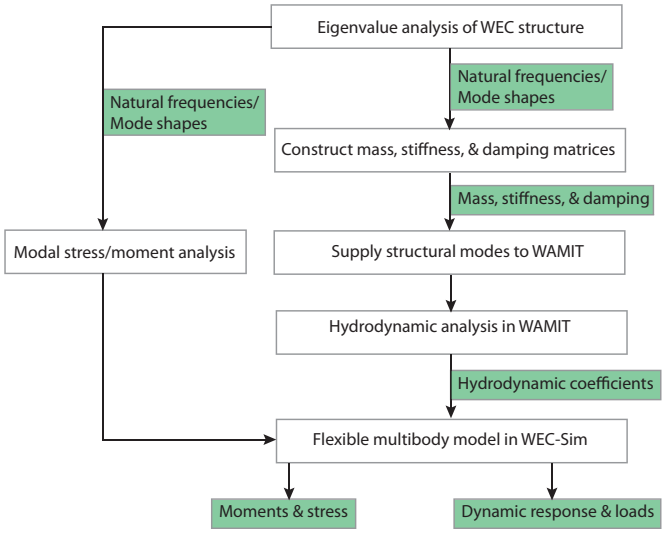

Fig. 1. Process of a structural-fluid analysis of WEC devices

IV. Finite Element Modeling

Finite element models of the barge and the column are created in ANSYS as shown in Fig. 2 and Fig. 3, respectively. Both models were built using beam elements (BEAM188) with three nodes per element. Mesh convergence studies were performed, resulting in a total of 80 beam elements for each structures. The free-free boundary conditions is applied to the barge model and the first four modes are then calculated with modal analysis. For the column, free-fixed boundary conditions are used to model the rigid connection to the seafloor, and modal analysis is used to obtain the first four modes. Although both structures could potentially be modeled with either beam or solid elements, the beam-element model is advantageous, in this application, because the element rotational DOFs may be exported along with the load and moment distributions. The modal mass and stiffness matrices, $\overline{\mathbf{M}}_f = \mathbf{\Phi}^T \mathbf{M}_f \mathbf{\Phi}$ and $\overline{\mathbf{K}}_f = \mathbf{\Phi}^T \mathbf{K}_f \mathbf{\Phi}$, as input in WAMIT, are listed in Table II.

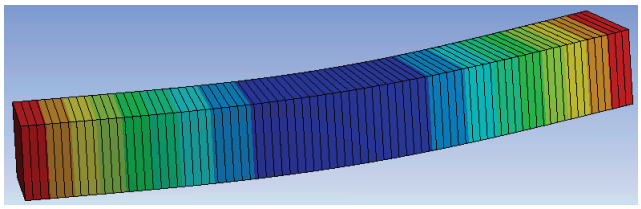

Fig. 2. Finite element model of the barge established in ANSYS

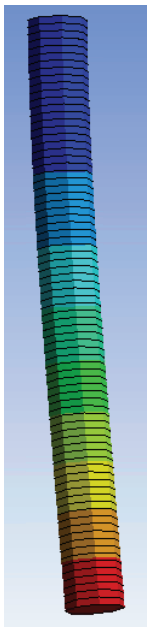

Fig. 3. Finite element model of the column established in ANSYS

TABLE II
Modal mass and stiffness properties of the barge and column, as calculated using FEA

Modes	Barge		Column	
	Mass (kg)	Stiffness (N/m)	Mass (kg)	Stiffness (N/m)
1^{st}	1.079×10^6	7.904×10^6	6.077×10^6	1.447×10^7
2^{nd}	1.210×10^6	8.267×10^6	4.383×10^7	5.560×10^8
3^{rd}	2.392×10^6	8.821×10^6	2.741×10^8	4.223×10^9
4^{th}	1.831×10^6	9.597×10^6	4.664×10^8	1.560×10^{10}

V. Result correlation with high-fidelity codes and experimental data

The presented method is validated by correlating results with full-scale computational fluid dynamics analysis consid-

ering FSI in STAR-CCM+ and the frequency-domain analysis in WAMIT. STAR-CCM+ [13], one of the highest fidelity CFD-FEA codes, was utilized in this study. FSI is modeled by implicitly coupling the unsteady RANS solver with a FVA solver, within the same STAR-CCM+ simulation. WAMIT performs boundary element analysis for simulating WEC's linearized hydrodynamic response in the frequency-domain. The steps of using generalized body modes to estimate wave loads on deformable bodies are documented in the WAMIT user manual [7]. Details on these two computational models of the studied articles are discussed in [1].

A. *Flexible barge*

The lowest bending mode shapes of the flexible barge are illustrated in Fig. 4. These modes were calculated using analytical formulation (Timoshenko beam theory) and FEA in ANSYS. The mode shapes have been normalized to unity such that $\mathbf{\Phi}^T\mathbf{\Phi} = \mathbf{I}$. The FEA predicts slightly larger deformation than the analytical approach in particular for higher modes because the finite element model considers the cross-couplings among different DOFs while the analytical approach does not. This cross-coupling is not negligible for flexible bodies. These modes in Fig. 4 were selected as candidate flexible body DOFs in WAMIT. WAMIT calculates the response of these flexible DOFs directly in the frequency-domain. It also provides associated hydrodynamic coefficients, which are later used in the time-domain model built in WEC-Sim.

Response amplitude operator (RAO) and bending stress of the proposed model for the flexible barge are compared against WAMIT and STAR-CCM+ in Figs. 5 and 6, respectively. From Fig. 5, it is evident that only the first two bending modes are significant for the barge. Good agreement among three approaches is evident and the result correlation between WAMIT and WEC-Sim is excellent. Table III compares the values of bending RAOs at the aforementioned four modes between WAMIT and WEC-Sim at wave period of 7.5 s. The largest error is less than 1.4% for the third and fourth modes. The error at the first dominating mode is less than 0.5%. The maximum RAO for the bending DOF occurs at 7.5 s wave period near where the pitch DOF reaches the maximum and heave DOF is the minimum. This phenomena could be a result of the interaction between flexible and rigid DOFs.

TABLE III
RESPONSE AMPLITUDE OPERATOR AT WAVE PEAK OF 7.5 s

Mode Number	WAMIT	WEC-Sim	Relative Error, %
1	1.74703E-01	1.74141e-01	-0.3221
2	1.63224E-02	1.63089e-02	-0.0827
3	4.40166E-04	4.46115e-04	+1.35
4	1.43094E-04	1.44575e-04	+1.03

Fig. 6 compares the maximum bending stress on the top of the barge along its length between the WEC-Sim and STAR-CCM+ at wave periods of 5, 7.5, 10 and 12 s. The agreement between these two approaches is reasonably well. The stress profiles over the barge length is nearly parabolic, primarily

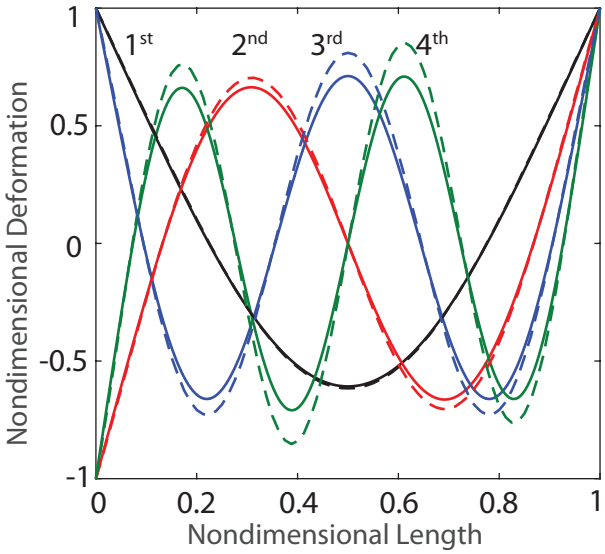

Fig. 4. Modes shapes of the barge calculated using analytical (——) and FEA (- - -) models

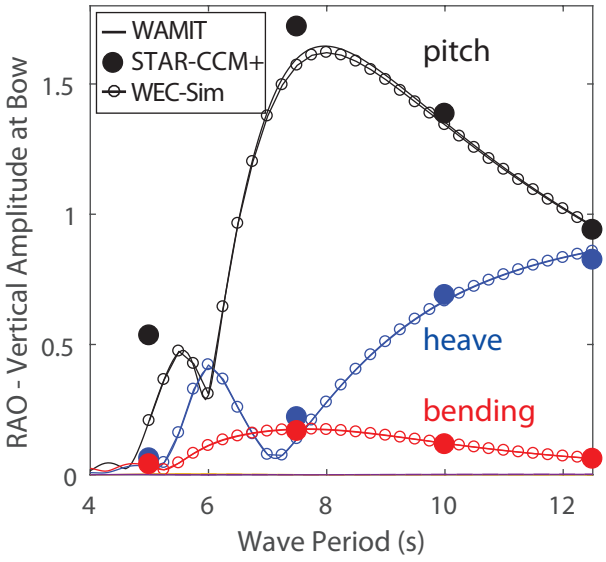

Fig. 5. RAO of the vertical displacement of the barge.

driven by the first mode in Fig. 4. At wave periods of 5 s and 12.5 s, the stress profiles include the effects of the second and higher modes.

B. *Flexible column*

Representing a single point absorber, the bottom of the column is considered fixed to the sea bed. Therefore, a clamped-free boundary condition is applied for the modal analysis. The lowest bending mode shapes of the flexible column calculated using the analytical and FEA approaches are illustrated in Fig. 7. The Timoshenko beam theory predicts almost the identical modal response of the column as FEA in ANSYS. Because the column is much stiffer than the barge, the cross-coupling among different DOFs is very little. Thus,

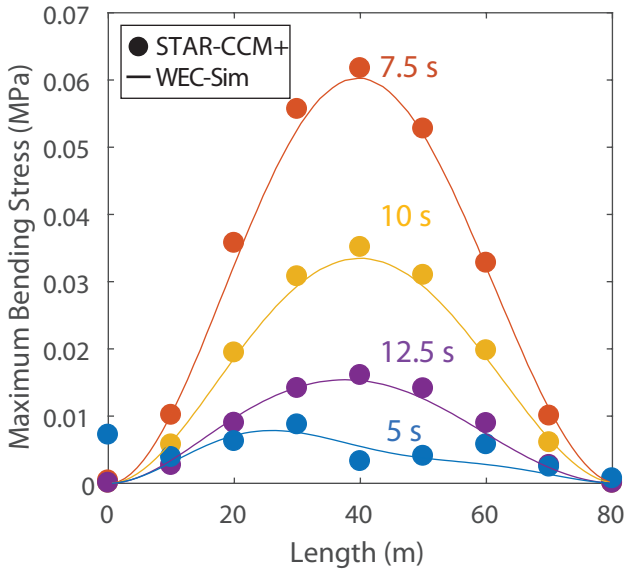

Fig. 6. Maximum bending stress amplitude along the barge at various wave periods

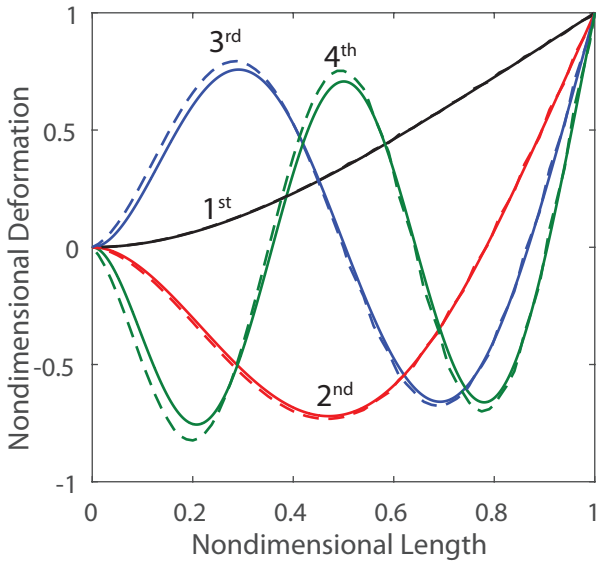

Fig. 7. Modes shapes of the column calculated using analytical (——) and FEA (- - -) models

the analytical results of the column match FEA results very well.

RAO of the proposed model for the flexible column is compared against WAMIT and STAR-CCM+ in Fig. 8. Viscous damping effects with $C_D = 1$ along the structure have be considered for the column case. As shown in Fig. 8, the first bending mode dominates the response for the column compared to higher modes (at least one order of magnitude higher) and reaches the maximum near wave period of $8.4\,s$. The result correlation among all three approaches is excellent.

Fig. 9 compares the bending stress profiles of the column along its height among WEC-Sim, WAMIT, and STAR-CCM+ at wave periods of 5.0, 6.7, 8.4, and $10.1\,s$. The agreement among all three approaches is good. The stress profiles are primarily determined by the first bending mode in Fig. 7 with small effects from higher modes. Small differences are present between the high fidelity STAR-CCM+ results and generalized body modes approach in WAMIT and WEC-Sim particularly near the top of the column. There are multiple reasons that contribute to the result differences. For instance, STAR-CCM+ model considers nonlinear wave effects while the other two do not, and STAR-CCM+ requires longer transient time to reach system's steady state. Additional discussions on the potential causes can be found in [1].

Fig. 10 compares the time-history of the oscillating bending stress of the column calculated using WEC-Sim and STAR-CCM+ at wave period of $6.7\,s$ under a regular wave with a time-ramp till $50\,s$. The agreement between these two approaches is reasonable well with slightly stronger oscillation in STAR-CCM+ results. Being able to calculate these stress cycles in the time-domain is an important step for the life calculations of WEC structures.

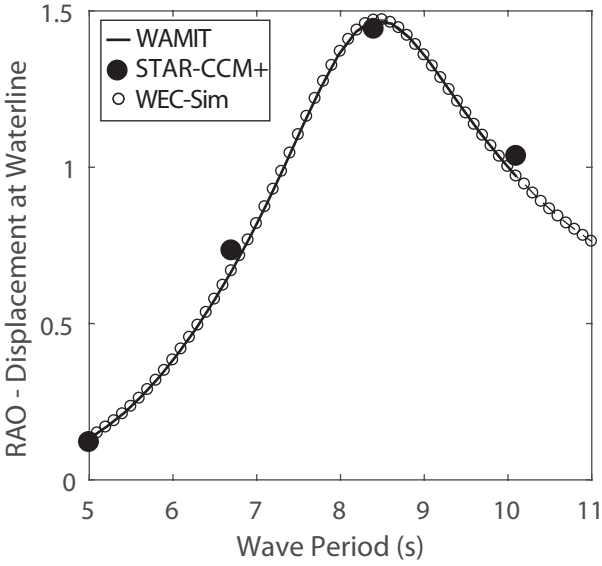

Fig. 8. RAO of the column displacement at the waterline for the first four bending modes

VI. Conclusions

A flexible multibody dynamics modeling approach is formulated and implemented in the open-source, time-domain simulation tool of WECs, WEC-Sim. This time-domain approach considers the structural flexibility of WEC components and provides a fast solution for WEC dynamic response, stress, and loads under the effects of wave loading.

This method is applied to two representative structures to calculate dynamic response and bending stress. Results calculated using the presented method are correlated with full-scale computational fluid dynamics analysis considering the fluid-structure interaction and the counterparts of the frequency-

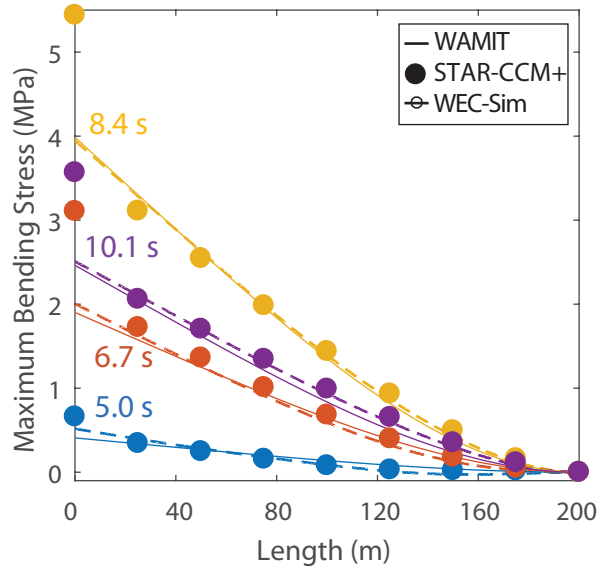

Fig. 9. Bending stress profiles of the column at wave periods of $5.0\,s$, $6.7\,s$, $8.4\,s$, and $10.1\,s$

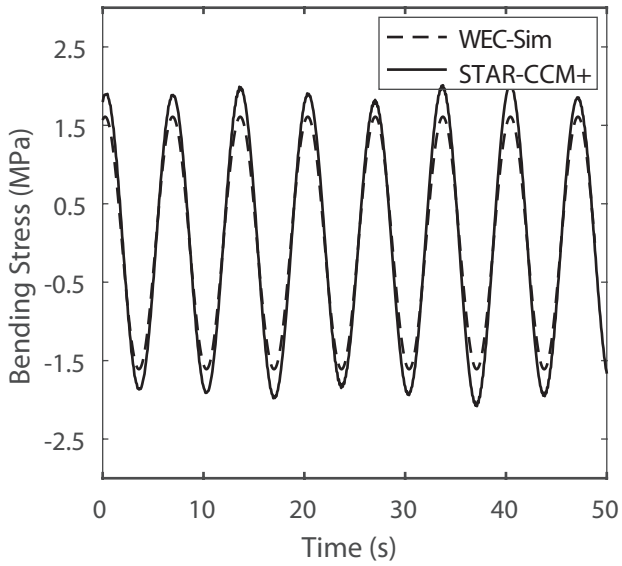

Fig. 10. Bending stress profiles of the column at wave periods of $6.7\,s$ at $25\,m$ from the column top

domain analysis. The agreement among these approaches is reasonably well.

Future research will be focused on using this method to simulate WEC devices with multiple bodies. It is also important to consider non-linear wave forces, mooring forces, and PTO forces in order to predict realistic responses and loads during WEC operation. A sensitivity study on the require number and types of candidate modes will be conducted for improving result accuracy. Finally, this study will become part of the WEC design-loads/extreme-condition-model framework [14] and WEC fatigue life calculation.

ACKNOWLEDGEMENT

This work was supported by the U.S. Department of Energy under Contract No. DE-AC36-08GO28308 with the National Renewable Energy Laboratory. Funding for the work was provided by the DOE Office of Energy Efficiency and Renewable Energy, Wind and Water Power Technologies Office.

REFERENCES

[1] J. van Rij, Y.-H. Yu, and Y. Guo, "Structural loads analysis for wave energy converters," in *Proc. of the 36th International Conference on Ocean, Offshore & Arctic Engineering*, Trondheim, Norway, 2017.

[2] E. Watanabe, C. M. Wang, T. Utsunomiya, and T. Moan, "Very large floating structures: Applications, analysis, and design," Centre for Offshore Research and Engineering, Tech. Rep., 2004.

[3] A. F. D. O. Falcão, "Wave Energy Utilization: A Review of the Technologies," *Renewable and Sustainable Energy Reviews*, vol. 14, pp. 899–918, 2010.

[4] B. Drew, A. R. Plummer, and M. N. Sahinkaya, "A review of wave energy converter technology," *Proc. IMechE*, vol. 223, pp. 887–902, 2009.

[5] K.-H. Kim, J.-S. Bang, J.-H. Kim, Y. Kim, S.-J. Kim, and Y. Kim, "Fully coupled bem-fem analysis for ship hydroelasticity in waves," *Marine Structures*, vol. 33, pp. 71–99, 2013.

[6] J. N. Newman, "Wave effects on deformable bodies," *Applied Ocean Research*, vol. 16, pp. 47–59, 1994.

[7] *WAMIT User Manual, Version 7.2*. Chestnut Hill, MA: Wamit, Inc. and Massachusetts Institute of Technology, 2016.

[8] R. Taghipour, T. Perez, and T. Moan, "Time-domain hydroelastic analysis of a flexible marine structure using state-space models," *Journal of Offshore Mechanics and Arctic Engineering*, vol. 131, 2009.

[9] R. Taghipour and T. Perez and T. Moan, "Hybrid frequency-time domain models for dynamic response analysis of marine structures," *Ocean Engineering*, vol. 35, pp. 685–705, 2008.

[10] Z. Yu and J. Falnes, "State-space modelling of a vertical cylinder in heave," *Applied Ocean Research*, vol. 17, pp. 265–275, 1995.

[11] Y.-H. Yu, M. Lawson, K. Ruehl, and C. Michelen, "Development and Demonstration of the WEC-Sim Wave Energy Converter Simulation Tool," in *2nd Marine Energy Technology Symposium*, Seattle, WA, 2014.

[12] P. Fischer and W. Witteveen, "Integrated mbs-fe-durability analysis of truck frame components by modal stresses," in *Proc. ADAMS User Meeting*. ADAMS, 2000.

[13] CD-adapco, "User guide STAR-CCM+ Version 11.04," 2016.

[14] R. Coe, C. Michelen, A. Eckert-Gallup, Y.-H. Yu, and J. van Rij, "Wdrt: A toolbox for design-response analysis of wave energy converters," in *Proceedings of the 4th Marine Energy Technology Symposium*, Washington, DC, 2016.